Asymmetry Phenomenon of Log-Periodic Dipole Antennas

KEITH G. BALMAIN, MEMBER, IEEE, AND JOSEPH N. NKENG, MEMBER, IEEE

Abstract—**The existence of asymmetric resonant modes on standard log-periodic dipole antennas is established experimentally. These modes are characterized by sharply-resonant side radiation sometimes accompanied by reduction in front-lobe gain. The resonances occur at frequencies whose relationship is approximately log-periodic. In a single antenna the resonant modes are excited by any structural asymmetry, while in an *E*-plane array each individual antenna excites the others asymmetrically. The resonances can be eliminated by the addition of lossy material to appropriate parts of the antenna. Qualitatively the phenomenon is explained in terms of transmission-line resonances along the two-wire lines formed by adjacent dipoles. Automated swept-frequency far-field measurement techniques were employed throughout, and their worth is clearly established for broadband antenna research and development.**

INTRODUCTION

LOG-PERIODIC dipole antennas (Fig. 1) have been used extensively since 1960 when their properties were described by Isbell [1], whose work was followed by the detailed analysis of Carrel [2]. Descriptions of these early developments are included in the survey articles by Dyson [3], Elliott [4], Mayes [5], and Jordan *et al.* [6], as well as in the book by Rumsey [7]. The subsequent development of computer-aided techniques contributed to a number of significant analyses of log-periodic dipole antennas, examples of which are the works by Cheong and King [8], Wolter [9], DeVito and Stracca [10], [11], and Sinnott [12].

A relatively recent development has been the observation and study of sharply-resonant anomalies in the electrical characteristics of log-periodic dipole antennas. High-level resonant back-lobe radiation coupled with front-lobe distortion was observed by Bantin and Balmain [13] at frequencies where the half-wavelength dipole and the short-circuit termination (the clamp at the large end of the antenna) are separated by a multiple of a half-wavelength measured along the feeder. Near the half-wavelength element is a stop-region [6] which behaves approximately as a short circuit. Therefore the section of feeder between the half-wavelength element and the large-end clamp can be regarded simply as a transmission-line resonator excited by whatever energy leaks past the radiating region and manages to penetrate the stop region. Because reflection from the end clamp is necessary for the existence of this resonance,

Manuscript received September 16, 1975; revised January 5, 1976. This work was sponsored in part by the Defence Research Board of Canada under Grant 9510-70 and in part by the National Research Council of Canada under Grant A-4140.

K. G. Balmain is with the Department of Electrical Engineering, University of Toronto, Toronto, Ont., Canada, M5S 1A4.

J. N. Nkeng was with the Department of Electrical Engineering, University of Toronto, Toronto, Ont., Canada. He is now with the School of Engineering, University of Yaounde, Yaounde, Cameroon, West Africa.

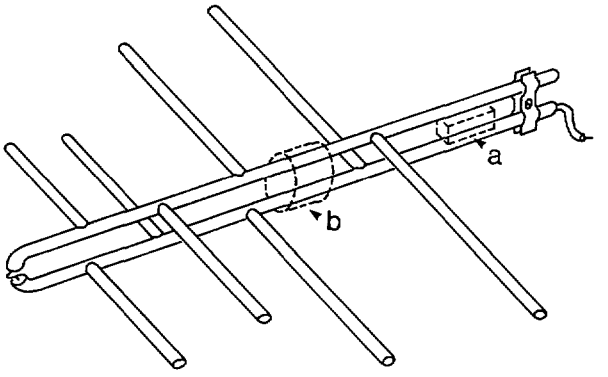

Fig. 1. Standard log-periodic dipole antenna. Shown are locations at which lossy material can be attached to eliminate (a) reflection anomalies and (b) asymmetry anomaly associated with largest cell (cell #1).

the resulting anomalies are sometimes called "reflection anomalies." Their excitation can be removed by increasing the efficiency of the radiating region. On the other hand, existing anomalies can be eliminated by decreasing the Q of the parasitic transmission-line resonator, using the lossy insert of Fig. 1(a). Both approaches have been mentioned in the literature [13], [14].

The phenomenon to be dealt with in this paper turns out to be quite unrelated to the one described above. For the sake of clarity it is best to begin with a qualitative postulate for the current distribution of an asymmetric resonant mode, and then to use this postulate as a point of reference to organize and explain the experimental data which follows.

A RESONANT-MODE POSTULATE

Consider first a two-wire transmission-line "half-wave" resonator (resonant when slightly shorter than $\lambda/2$) as shown in Fig. 2(a). Then imagine the two wires to be offset slightly as in Fig. 2(b). Subsequently, imagine the transmission line to be twisted in the middle as in Fig. 2(c), so that the resulting configuration can be regarded as one cell of a log-periodic antenna. After this distortion of the wires, it seems plausible that the half-wave resonance would continue to exist and that its current distribution and resonant frequency would not have changed greatly. It is much less certain that the resonance could retain its identity upon incorporation of the cell into a log-periodic antenna, as is suggested in Fig. 2(d), but such a proposition may well be a useful one to retain until firm evidence shows how much it needs to be modified.

If such a resonance could exist on an antenna, certainly it would not be excited in a symmetric antenna driven by a

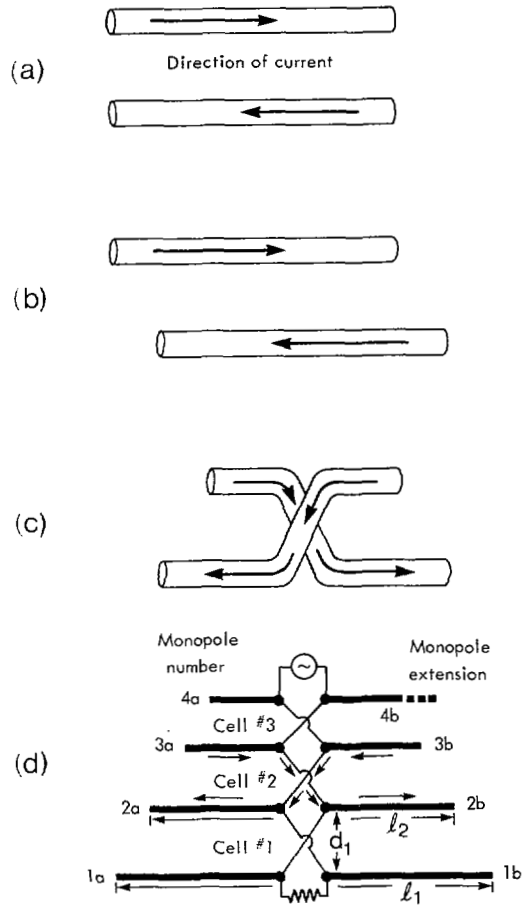

Fig. 2. Evolution of asymmetric resonance, showing (a) parallel-wire resonator, (b) offset parallel-wire resonator, (c) single cell, and (d) top view of antenna showing asymmetric resonance in cell #2. Note antenna parameters: $\tau = l_n/l_{n-1} = d_n/d_{n-1}$, $\sigma = d_n/2l_n$.

symmetric source such as the voltage generator of Fig. 2(d). For the reciprocal receiving-antenna case, an off-boresight incident wave would excite the resonance but the resonance would not contribute to the signal at the antenna terminals. Returning to the transmitting case, we can see that any asymmetry such as the monopole extension of Fig. 2(d) would excite the resonance and, once excited, the resonant current distribution would radiate appreciably from that section of the feeder lying within the resonant cell. Because the feeder also constitutes the mechanical support boom for the dipole elements, it is clear that the resonant-frequency radiation would appear to come partly from the boom and would therefore radiate to the side of the antenna.

Experimental Method

The primary method employed was that of swept-frequency far-field measurement, for both principal polarization and cross polarization. Point-contact crystal diode detectors were used; with them, the system amplitude response at selected frequencies was calibrated and found to be linear in decibels to within ± 0.2 dB, and variations over the whole frequency range were estimated to be less than ± 0.5 dB. The range antenna used was an anomaly-free log-periodic with a design frequency range of 0.5 to 3.0 GHz. The various antenna arrangements used are shown in Fig. 3. A typical procedure is to rotate the test antenna in steps of either 5°, 10°, or 30°, at each step making a graphical recording of the transmitted-signal amplitude as a function of frequency. For most of the arrangements shown, this procedure has to be limited to a 90° quadrant in order to avoid excessive overlapping of the lines on the graph. For the experiments to be described, the above procedure was fully automated.

The numbering system for elements and cells has already been indicated in Fig. 2(d). Each dipole is composed of two monopoles, numbered so that they can be referred to individually. In this paper, the term "cell" includes two adjacent dipoles and the section of feeder between them. Every antenna used in this study had seven dipoles and therefore six cells. The value $\tau = 0.89$ was used along with a structure bandwidth of 2 : 1. The half-wavelength frequencies of the dipoles were 550, 617, 693, 778, 873, 979, and 1100 MHz; exceptions to this were the antennas exhibiting "accidental asymmetry," for which the corresponding frequency range was from 500 to 1000 MHz.

Experiments

Monopole Extension

Deliberate asymmetric distortion was applied to a precisely-constructed antenna by means of various monopole extensions. The antenna in question (designated #21) had $\tau = 0.89$ and $\sigma = 0.15$. The undistorted antenna had a very regular E-plane front-quadrant pattern as can be seen in Fig. 4(a). Figs. 4(b) through (d) show the anomalous effects of progressive extension of monopole #4a, effects which are remarkable because of their highly resonant properties. At the frequency of each pattern anomaly, radiation from the boom (side radiation) is the predominant effect although depression of the front lobe occurs if a resonance is excited with sufficient strength. It should be noted that no anomalies occur above the nominal half-wavelength frequency of the distorted dipole (778 MHz), presumably because in a normal log-periodic antenna negligible current flows in the dipole above that frequency. Similar effects were produced by bending a monopole or by sliding a metal sleeve over it. Symmetric distortion was also tried by extending equally the two ends of a dipole; no resonant anomalies appeared, the only pattern degradation being slowly-varying with frequency.

Accidental Asymmetry

A number of the antennas tested had been constructed originally in a rather imprecise manner using thin brass wire for the dipoles, which had a length-to-diameter ratio of about 145. Over a period of several years these antennas had been used in a large number of laboratory experiments with the result that the majority of their elements had become slightly bent. Thus their asymmetry was somewhat random in nature and degree, and quite impossible to characterize precisely. However, it can be said that the maximum departure from monopole straightness was of the order of the wire radius, and that the deflection of the

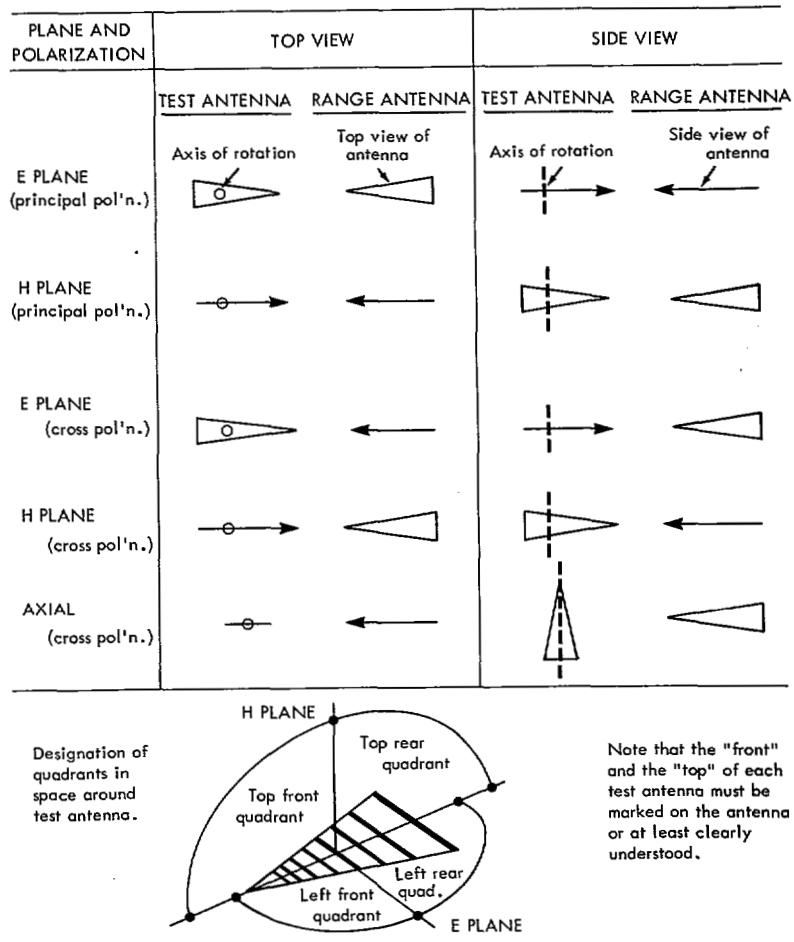

Fig. 3. Antenna far-field measurement conventions.

end of a monopole from its proper position was rarely more than a wire diameter. For one such antenna (#18), the *E*-plane and axial patterns are shown in Fig. 5. The axial pattern is particularly interesting, not only because the anomalous radiation peaks are high and sharp, but also because the radiated field at each peak is independent of the angle of rotation of the antenna. Clearly at these peaks the radiation must be coming from a net unbalanced current along the antenna axis as suggested by the postulate already presented. Also according to the postulate, the number of anomalies (6) is equal to the number of cells.

Similar patterns are shown in Fig. 6 for an antenna (#7) whose elements are not so closely spaced as in the foregoing example. In the present example there are only five side-radiating asymmetry anomalies, a reduction in number with increasing σ which turns out to be the beginning of a trend (to be discussed farther on in greater detail). This antenna exhibits an additional peculiarity, a "notch" in the front lobe at a frequency just above the fifth asymmetry anomaly; this notch is one of the reflection anomalies discussed in the Introduction.

From the *E*-plane, front-quadrant patterns presented so far, it can be seen that the anomalous radiation and the primary radiation appear to combine in a manner that is sometimes in-phase, sometimes out-of-phase, and sometimes approximately in quadrature. However, for any one anomaly, as the antenna rotates there seems to be little change in the apparent relative phase between anomalous and primary radiation. Consequently the phase center for the anomalous radiation must be very nearly coincident with the phase center for the primary radiation.

If the anomalous radiation comes from a current distribution like the one shown in Fig. 2(c) or (d), then in an *E*-plane pattern the phase of this radiation will reverse as the antenna is rotated through the boresight direction while the phase of the primary radiation remains essentially unchanged. The effect of this can be seen in Fig. 7, in which all the anomalies in the *left* front quadrant happen to appear as simple additions or subtractions. Going to the *right* front quadrant, we see that an additive anomaly changes to a subtractive anomaly and vice-versa, as expected. It is worth noting that a polar pattern taken on one of these anomaly frequencies would reveal an off-boresight "skewing" of the front lobe.

The anomaly frequencies appear to be log-periodically arranged in frequency but their average ratio turns out to be less than τ, and furthermore for most antennas tested the number of anomalies is *less* than the number of cells. This effect becomes more pronounced as σ increases, as can be seen from Table I. This suggests in general that a given resonance occupies slightly more than one cell and therefore that the postulate presented here holds with accuracy

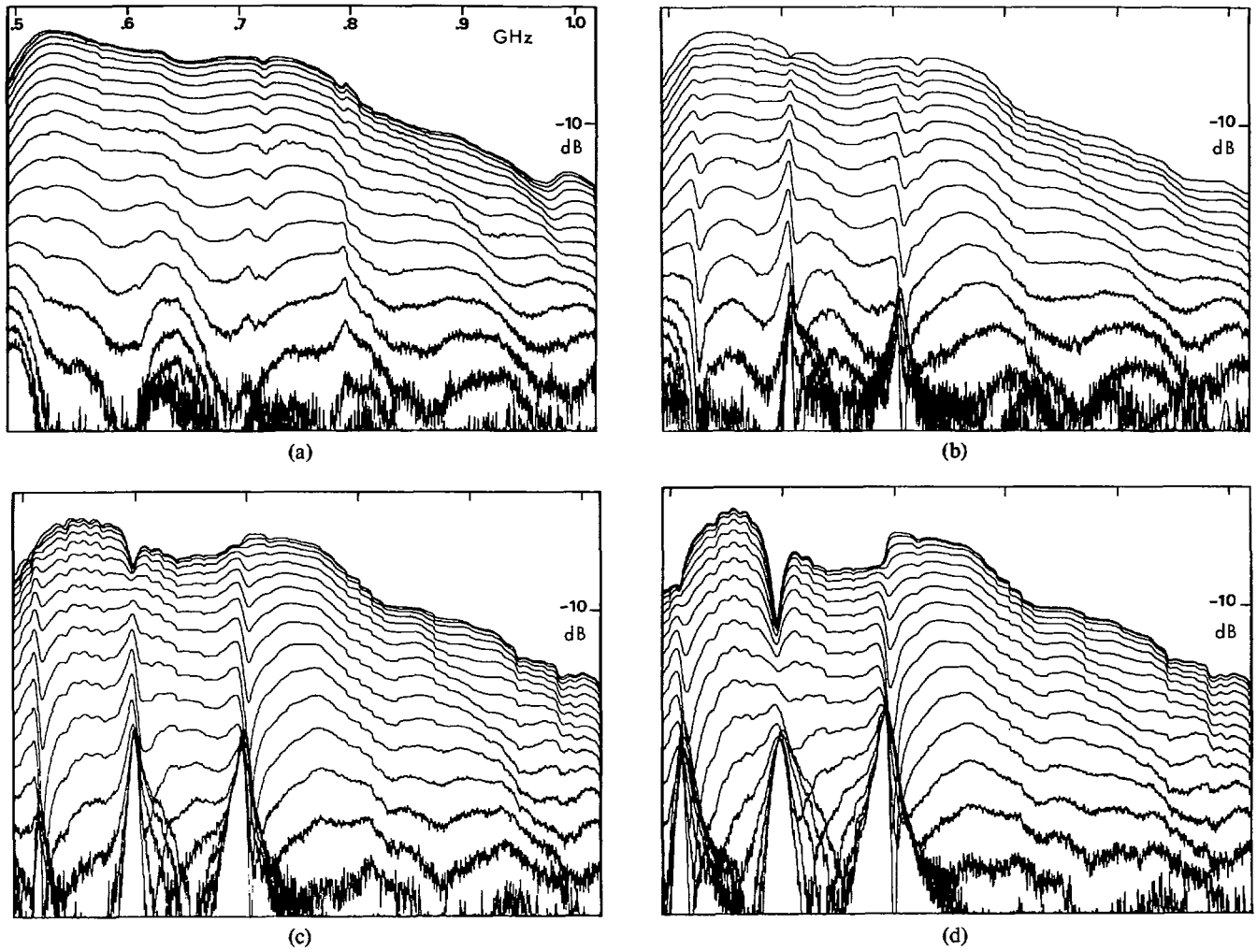

Fig. 4. Swept-frequency far-field patterns of antenna #21, displaying effect of extending monopole #4a by (a) zero, (b) 2.4 percent (0.5 cm), (c) 4.7 percent (1.0 cm), and (d) 9.4 percent (2.0 cm). Percentages are with respect to total dipole length. *E*-plane, principal polarization, left front quadrant with 5° rotation increments is shown; top curve is boresight measurement and usually lowest-level curve is at 90° to boresight (side radiation). Top border is 0 dB reference for linear-in-dB vertical scale.

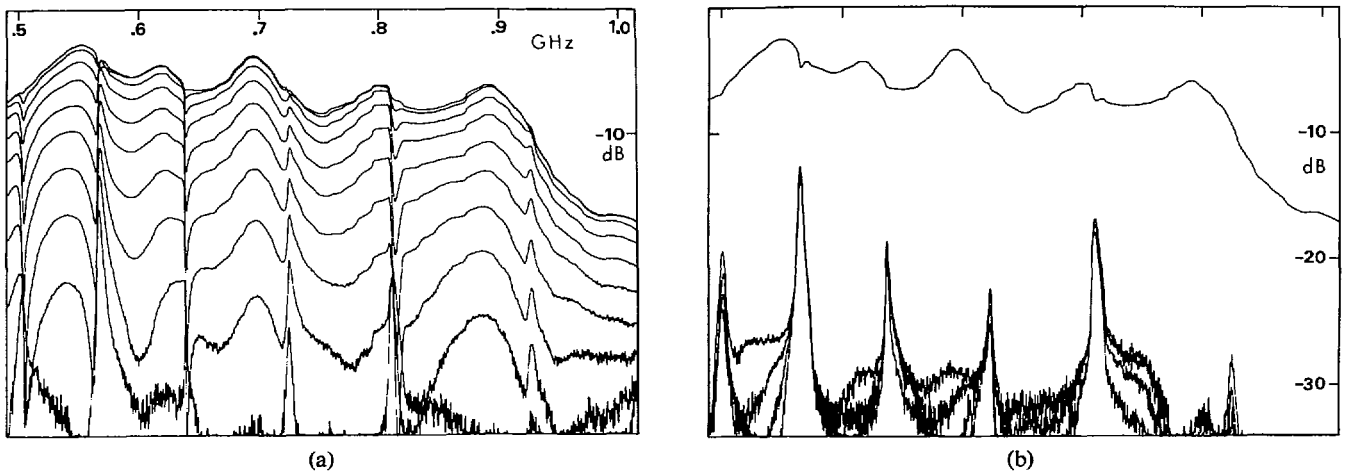

Fig. 5. Effect of accidental asymmetry in antenna #18 with $\sigma = 0.019$. In (a) is *E*-plane, principal polarization, right front quadrant with 10° increments and in (b) is axial plane, cross polarization, bottom right quadrant with 30° increments and with boresight curve included for reference.

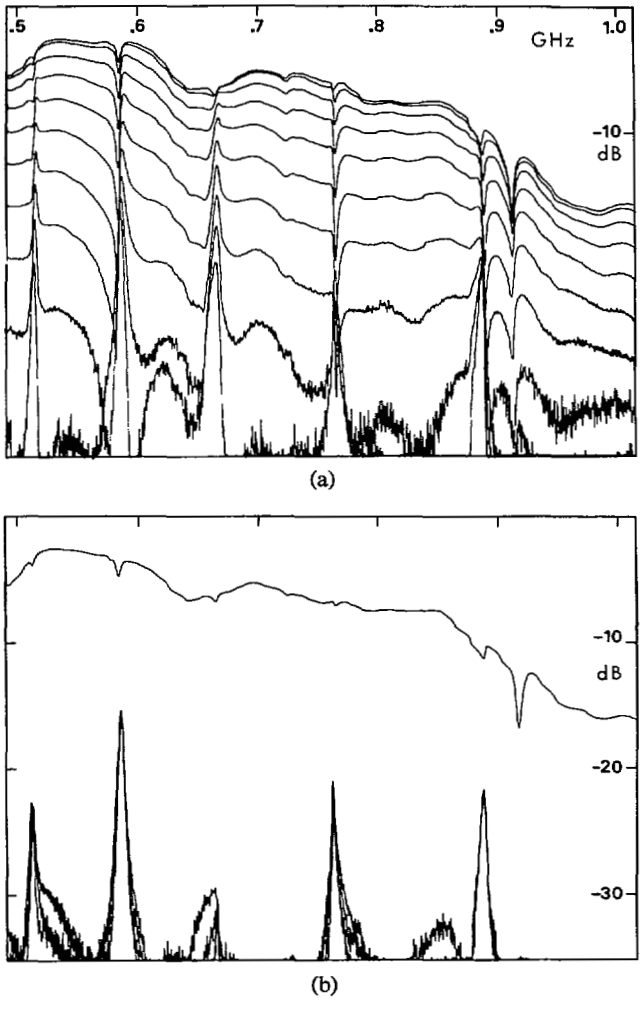

Fig. 6. Effect of accidental asymmetry in antenna #7 with $\sigma = 0.046$. Other specifications are same as for Fig. 5.

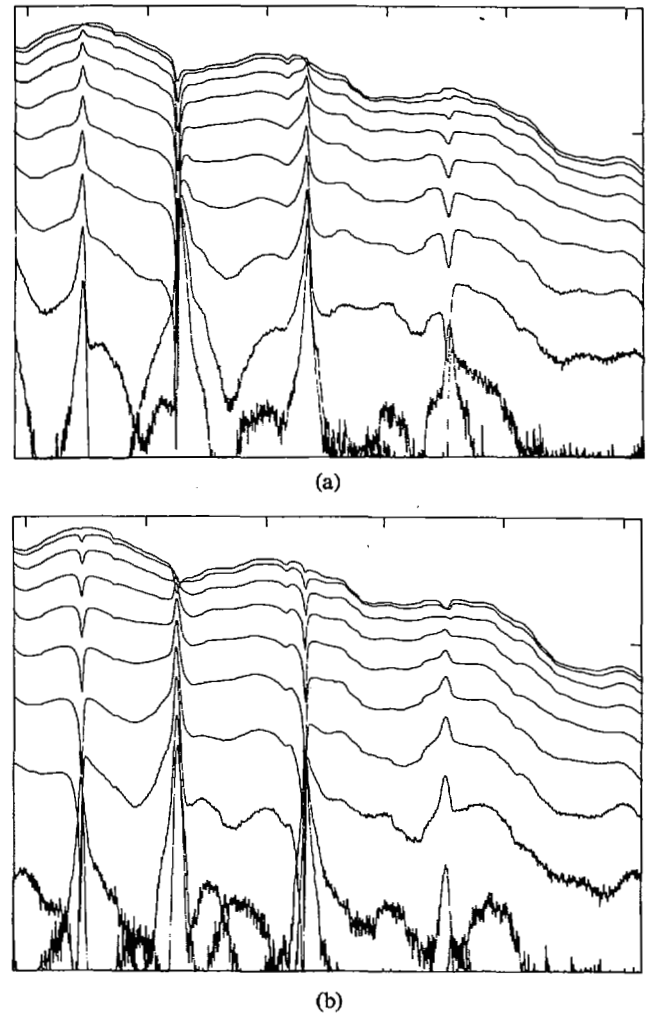

Fig. 7. Left front quadrant (a), and right front quadrant (b), for *E*-plane, principal-polarization measurement of antenna #14 with $\sigma = 0.073$. Axes are same as in foregoing figures.

TABLE I
AVERAGE ANOMALY FREQUENCY RATIO AND NUMBER OF ANOMALIES, AS FUNCTIONS OF ANTENNA PARAMETERS τ AND σ

Antenna Identification Number	Average Anomaly Frequency Ratio	τ	σ	Number of Anomalies Seen
16	0.828	0.89	0.15	3
17	0.854	0.89	0.10	4
14	0.859	0.89	0.073	5
19	0.861	0.89	0.073	5
10	0.863	0.89	0.056	5
7	0.866	0.90	0.046	5
13	0.867	0.89	0.073	5
9	0.872	0.90	0.038	5
8	0.873	0.89	0.025	5
18	0.877	0.89	0.019	6

only for antennas which are highly compressed (antennas with small σ).

The anomalous resonances affect the input impedance as well, appearing as very small loops or cusps in a swept-frequency Smith-chart presentation. Such loops or cusps are characteristic of weakly-coupled resonators, so their appearance is consistent with the postulated resonance mechanism.

Scattering

If a log-periodic antenna is used as a scatterer of electromagnetic waves, then it is possible to detect the anomalous resonances without any need for structural asymmetry. Furthermore, scattering techniques can be used to find the resonant frequencies of single cells and also of multicell structures which resemble antennas but which do not have the proper feed cable connections to permit their use as antennas. This latter case is shown in Fig. 8 with a multicell scatterer located between cross-polarized range antennas. For such an experiment a typical swept-frequency record of transmitted signal magnitude is shown in Fig. 9(a). Similar results were obtained with actual antennas, the transmission peaks occurring at exactly the same frequencies as the anomalies previously described. Also using the scattering technique, one can measure the resonant frequency of a single cell, a typical result being shown in Fig. 9(b).

The scattering experiments are introduced here not merely as another means to identify anomalous resonances, but also to trace the changes in resonant frequency through the steps illustrated in Fig. 2, as the two-wire transmission-line resonator is modified in shape and eventually incorporated

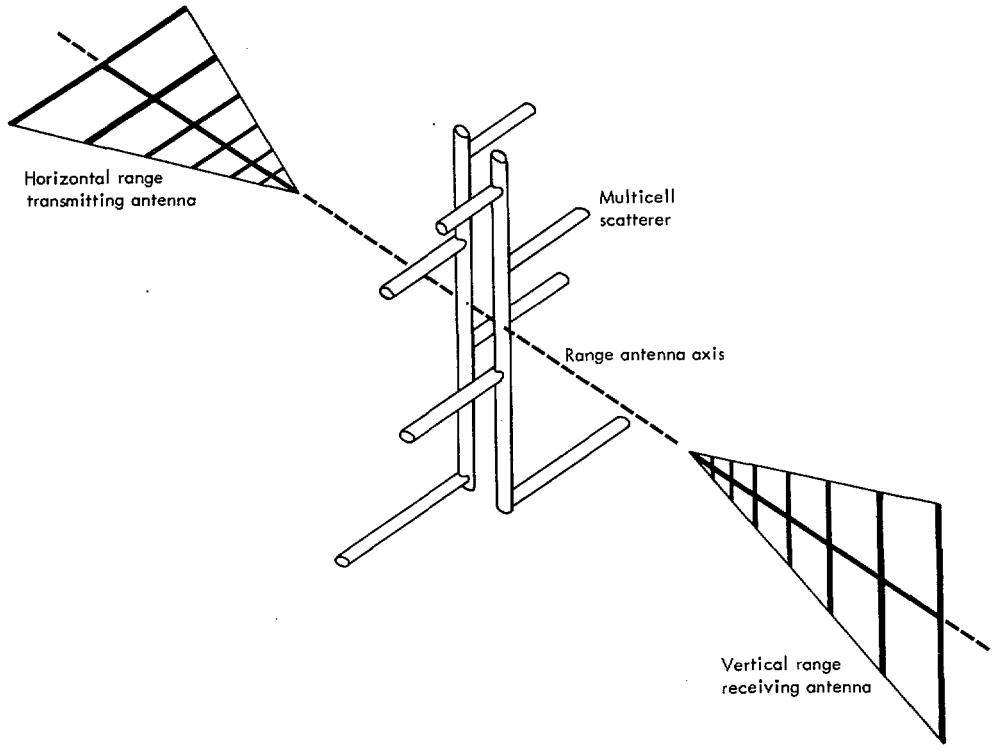

Fig. 8. Scattering experiment involving polarization transformation by multicell scatterer.

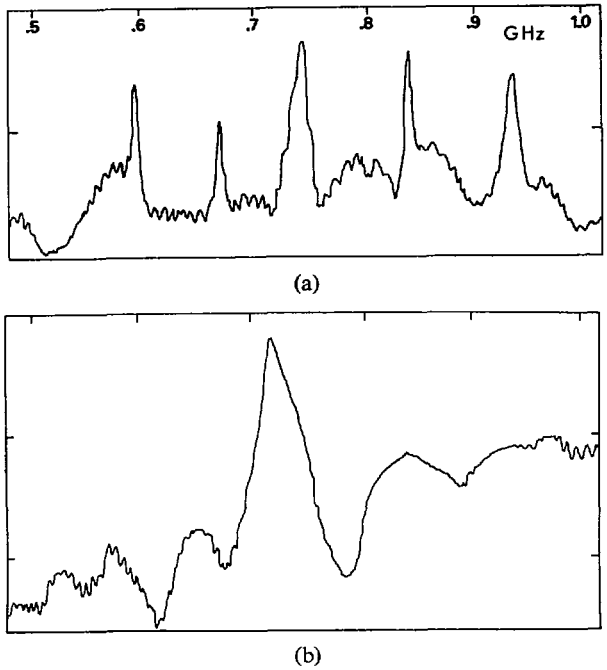

Fig. 9. Transmitted signal magnitude in scattering experiment. Part (a) is for seven-dipole multicell scatterer having $\tau = 0.9$, $\sigma = 0.04$, feeder spacing of 1.2 cm, wire diameter of 4.76 mm, and longest dipole half wavelength at 600 MHz. Part (b) is for single cell with wire segment lengths of 8, 2, and 10 cm for total of 20 cm which is half wavelength at 750 MHz; separation between wire planes is 2.2 cm (see Fig. 2(c) for sketch of single cell).

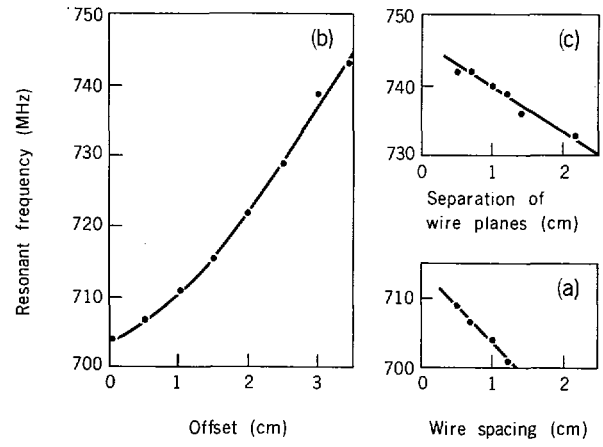

Fig. 10. Typical resonant frequency variations for (a) parallel-wire resonator 20 cm long, (b) offset, parallel wire resonator with wire spacing of 1 cm and 20 cm wire lengths, and (c) single cell with total wire length of 20 cm and segments of 8, 2, and 10 cm. Wire diameter of 4.76 mm applies for all cases.

as a cell in an antenna. A parallel-wire resonator, when located between the cross-polarized range antennas, produces a swept-frequency transmission graph similar to that in Fig. 9(b) but with a much sharper peak. For such a measurement, the two wires of the resonator lie transversely in a plane which contains the common axis of the two range antennas and which is oriented at 45° to the element planes of those two antennas. Typical resonance frequency variations for this case are indicated in Fig. 10(a). The offset parallel-wire resonator of Fig. 2(b) exhibits a well-defined resonance with a higher resonant frequency as indicated in Fig. 10(b). The single cell of Fig. 2(c) has a resonance with a lower Q and a range of resonant frequencies indicated in Fig. 10(c). All the measured points in Fig. 10 lie within a ± 3 percent frequency range, so for practical purposes it can be said that the resonance retains its identity throughout the process of transforming the two-wire resonator into the single antenna cell.

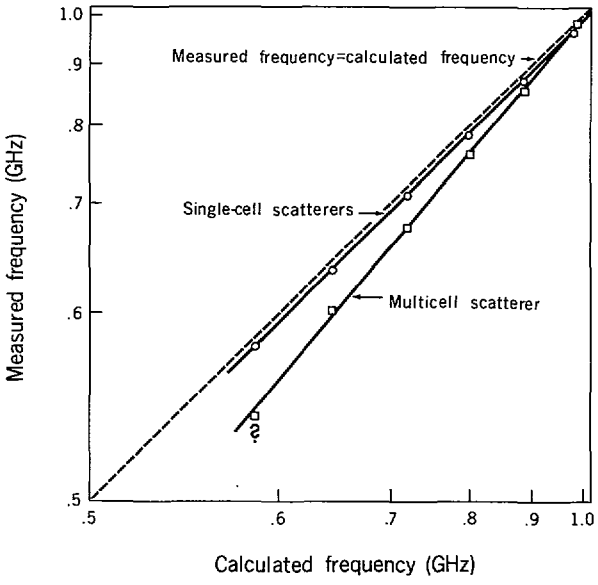

Fig. 11. Comparison of calculated and measured resonant frequencies for single cells, and for multicell scatterer of Fig. 9(a) with feeder spacing of 0.8 cm. Point marked (?) was difficult to observe, requiring re-orientation of scatterer to be measurable.

The resonant frequency of a single cell is usually about two percent lower than the theoretical resonance frequency, at which the total length of wire in either of its two conductors is a half wavelength. This relationship held true for a set of six individual log-periodically-scaled cells as indicated in Fig. 11. The same figure also shows the resonant frequencies of six similar cells when assembled to form a multicell scatterer (which was essentially a seven-dipole log-periodic antenna). For this particular case the lower resonant frequencies were changed by as much as 7 percent while the higher frequencies were changed hardly at all. Evidently the coupling between cells can influence the resonances appreciably.

Introduction of Lossy Material

In an attempt to locate and control the asymmetric resonance, a magnetically and electrically lossy, flexible material (Eccosorb FDS) was wrapped around both conductors of the antenna boom as shown in Fig. 1(b), each wrapping ahead of the $\lambda/2$ dipole reducing the forward gain by about 1 dB. In this manner, the lossy material was introduced into one cell at a time and for each such case the axial radiation (radiation from the boom) was measured. The result for a six-anomaly antenna (#18) is shown in Fig. 12 which displays unambiguously a one-to-one correspondence between wrapped cells and eliminated anomalies, precisely as one would expect if the postulate outlined in this paper were valid. However, the results for a five-anomaly antenna do not fall so neatly into place, as can be seen in Fig. 13. The one-to-one correspondence mentioned above seems at first to hold if one follows the wrapping procedure from either the low-frequency end or the high-frequency end, but the correspondence fails in the mid-frequency range. This supports the conclusion already arrived at following the discussion of Table I, that the asymmetric resonance currents spread out to occupy slightly more than one cell as σ increases. The same conclusion was reinforced by many other experiments, involving for example the element-by-element assembly of an antenna while tracking the resonance frequencies at each step in the assembly [15].

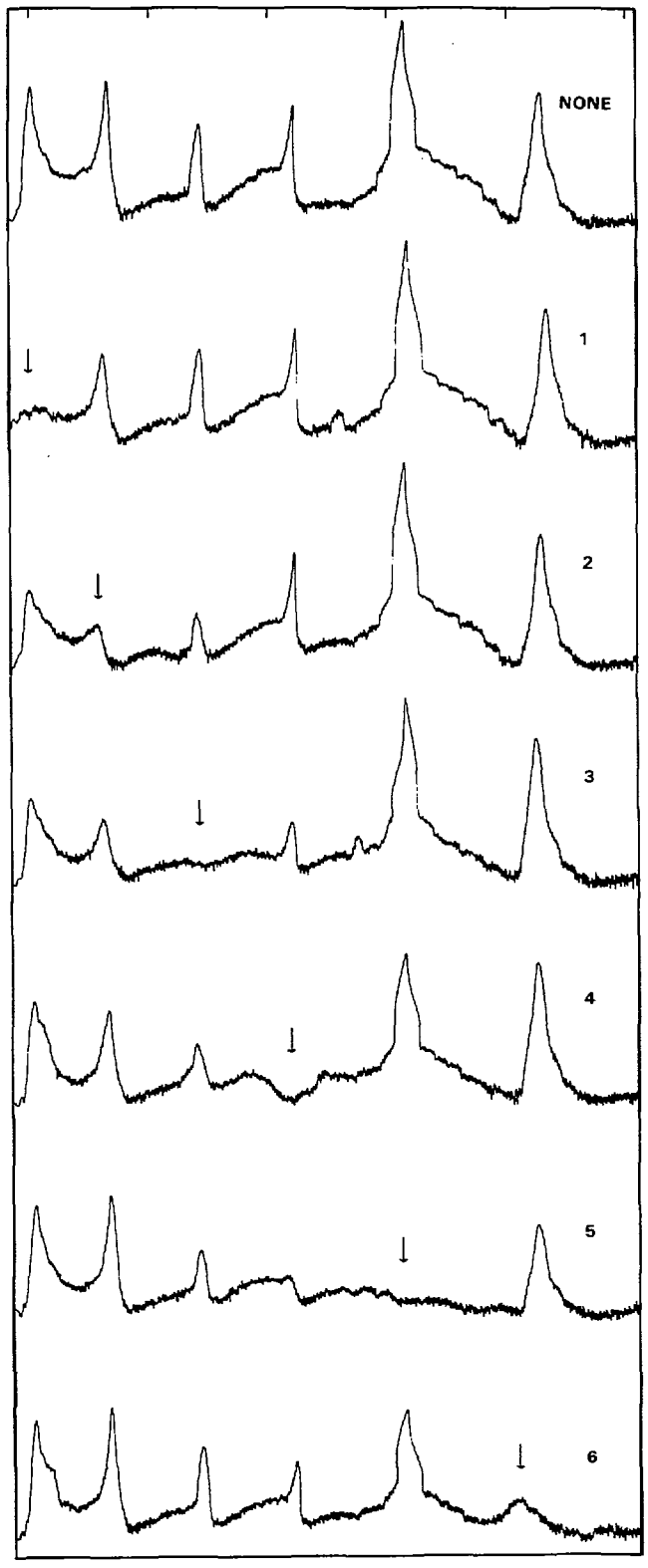

Fig. 12. Effect on side radiation of wrapping lossy material around feeder section of each cell in antenna $\neq 18$. Numbers at right indicate which cell has been wrapped. Arrows indicate anomaly most strongly affected. Horizontal frequency scale is same as in foregoing figures.

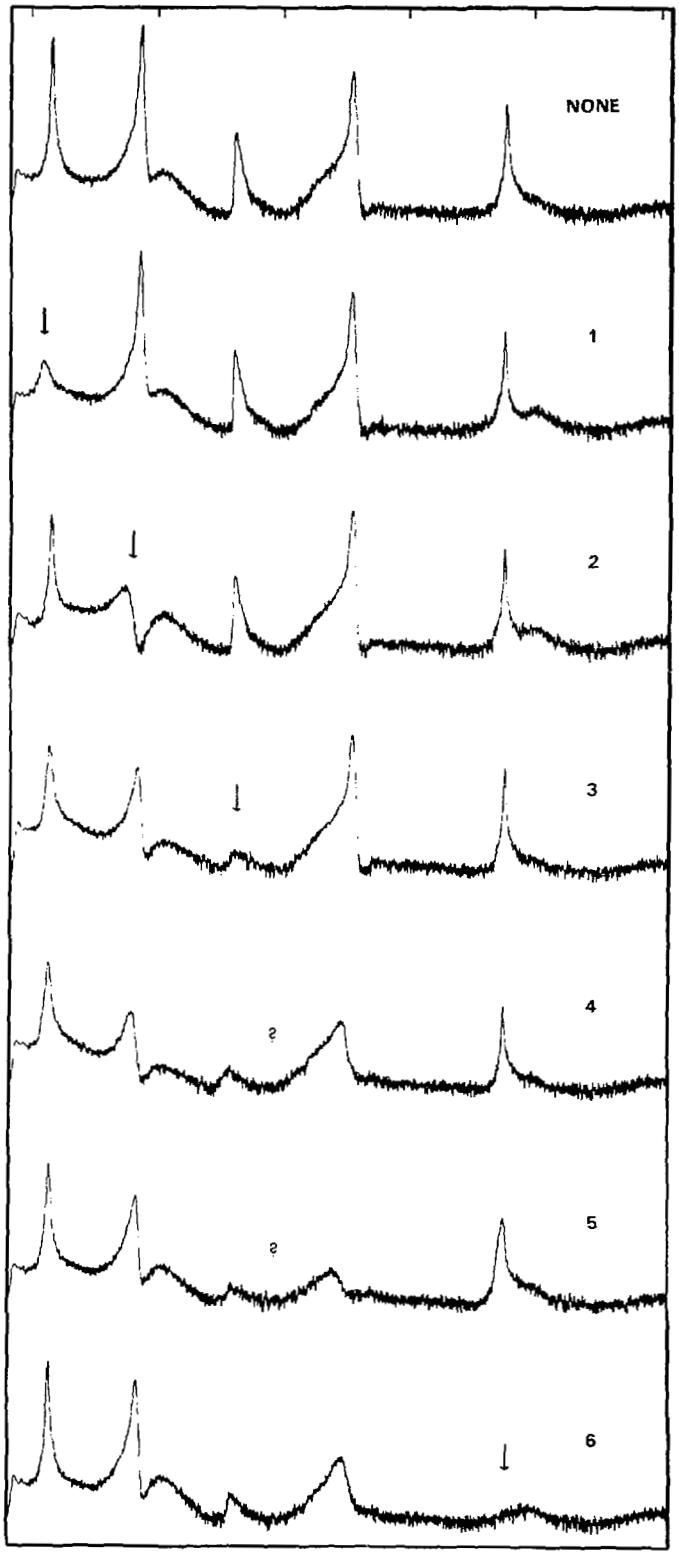

Fig. 13. Effect on side radiation of wrapping lossy material around feeder section of each cell in antenna #7. Remaining specifications are same as in Fig. 12.

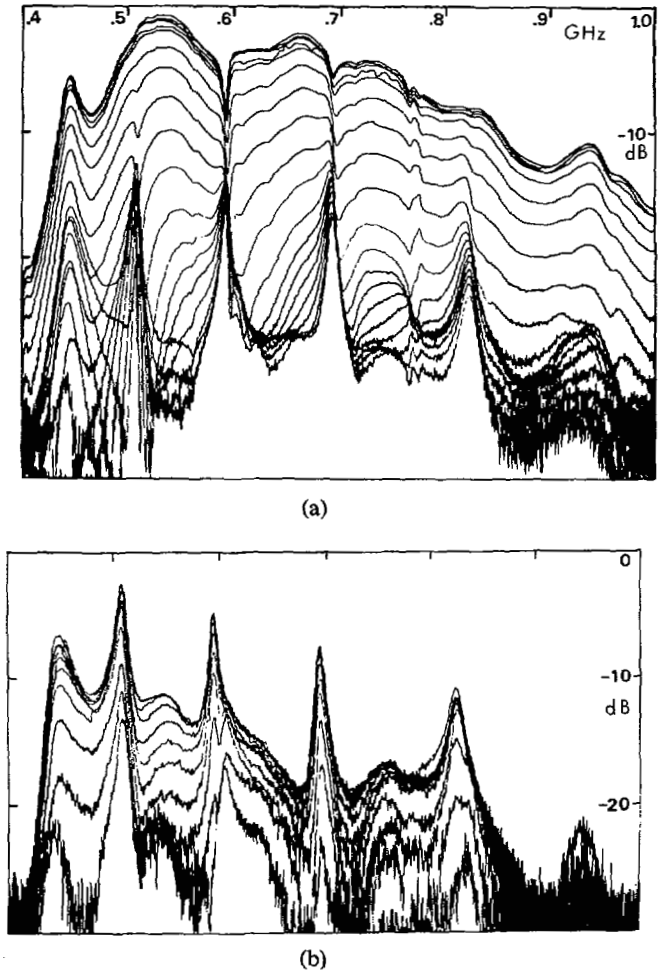

Fig. 14. Asymmetry anomalies in common-apex *E*-plane array, showing (a) *E*-plane front quadrant pattern, and (b) axial plane, single quadrant pattern. In array centers of half-wavelength dipoles were separated by 0.6 wavelength.

E-Plane Array

In a coplanar array (or *E*-plane array) of two log-periodic dipole antennas, the two antennas sometimes are arranged in a "common apex" configuration to maintain frequency independence in the array pattern. In such a configuration the normal radiating region of one antenna irradiates the anomalous resonance region of the other antenna, exciting exceptionally strong anomalies in spite of the fact that each antenna by itself may be perfectly symmetric. A case of this type is illustrated in Fig. 14 where the strong array anomalies are at the same frequencies as the individual antenna anomalies (which were in fact so small as to be almost undetectable). The introduction of lossy sheets between the halves of each antenna eliminates the anomalies completely but with the loss of a few decibels of gain [15]. The anomaly amplitudes are greatly reduced in a parallel-boom configuration but even then with close spacing the lower-frequency anomalies may persist [16]. Clearly all the above comments on *E*-plane arrays apply equally to vertically-polarized antennas over ground. As for *H*-plane arrays (horizontally-polarized antennas over ground), we have confirmed experimentally the intuitive expectation that they would not exhibit asymmetry anomalies (*H*-plane arrays have been studied both theoretically and experimentally by Kyle [17]).

It is important to note that very sharp and deep "gain reduction anomalies" were observed but not explained in a

study of E-plane arrays reported by Elfving and Miller [18], and described by Kuo [19]. It seems certain that their anomalies are the same as the asymmetry anomalies discussed in this paper.

Conclusions

Structural asymmetry causes resonant side radiation from log-periodic dipole antennas. This radiation arises from the excitation of a family of asymmetric resonances, each with currents occupying one to two cells of the antenna structure. Excitation of these resonances is also caused by asymmetric irradiation from other antennas in an E-plane array (including the image for an antenna over ground). The resonances can be eliminated by avoiding their excitation in the first instance, or as an afterthought by introducing enough lossy material to damp them out. The quantity of lossy material required and the resultant decrease in antenna gain both depend on the degree to which the resonances are excited in a given situation. Therefore the introduction of lossy material may not be a practical solution for an operational antenna. The phenomenon described here could be used to establish mechanical construction tolerances or tolerances on post-construction damage by relating either of them to tolerable limits on side-radiation or front-lobe skewing. The asymmetric resonances have a high Q and for that reason are easily excited, so that even the perching of a bird near one end of a dipole could be a source of difficulty!

The explanatory postulate put forward in this paper is rudimentary but nevertheless useful quantitatively for small σ and qualitatively for large σ. It is interesting to observe that, to the extent of the authors' knowledge, the asymmetric resonances could not have been predicted by any published theories of log-periodic dipole antennas because all these theories have assumed balanced feeder currents!

The use of an automated, swept-frequency far-field measurement system was essential in carrying out this research. Such a system should now be recognized as necessary in any program of research and development involving broadband antennas.

Acknowledgment

The authors thank J. F. Pope for the design and construction of the automated measurement system. Thanks are also expressed to D. Y. Z. Waung, V. Mozarowski, and A. Maraschiello for making relevant measurements.

References

[1] D. E. Isbell, "Log-periodic dipole arrays," *IRE Trans. Antennas Propagat.*, vol. AP-8, pp. 260–267, May 1960.
[2] R. L. Carrel, "The design of log-periodic dipole antennas," in *1961 IRE Int. Conv. Rec.*, vol. 1, pp. 61–75.
[3] J. D. Dyson, "A survey of the very wide band and frequency independent antennas—1945 to the present," *J. Research NBS-D, Radio Propag.*, vol. 66D, pp. 1–6, Jan.–Feb. 1962.
[4] R. S. Elliott, "A view of frequency independent antennas," *Microwave J.*, pp. 61–68, Nov. 1962.
[5] P. E. Mayes, "Broadband backward-wave antennas," *Microwave J.*, pp. 61–71, Jan. 1963.
[6] E. C. Jordan, G. A. Deschamps, J. D. Dyson, and P. E. Mayes, "Developments in broadband antennas," *IEEE Spectrum*, vol. 1, pp. 58–71, Apr. 1964.
[7] V. H. Rumsey, *Frequency Independent Antennas*. New York: Academic Press, 1966.
[8] W. M. Cheong and R. W. P. King, "Log-periodic dipole antenna," *Radio Sci.*, vol. 2, pp. 1315–1325, Nov. 1967.
[9] J. Wolter, "Solution of Maxwell's equations for log-periodic dipole antennas," *IEEE Trans. Antennas Propagat.*, vol. AP-18, pp. 734–741, Nov. 1970.
[10] G. De Vito and G. B. Stracca, "Comments on the design of log-periodic dipole antennas," *IEEE Trans. Antennas Propagat.*, vol. AP-21, pp. 303–308, May 1973.
[11] ——, "Further comments on the design of log-periodic dipole antennas," *IEEE Trans. Antennas Propagat.*, vol. AP-22, pp. 714–718, Sept. 1974.
[12] D. H. Sinnott, "Multiple-frequency computer analysis of the log-periodic dipole antenna," *IEEE Trans. Antennas Propagat.*, vol. AP-22, pp. 592–594, July 1974.
[13] C. C. Bantin and K. G. Balmain, "Study of compressed log-periodic dipole antennas," *IEEE Trans. Antennas Propagat.*, vol. AP-18, pp. 195–203, Mar. 1970.
[14] K. G. Balmain, C. C. Bantin, C. R. Oakes, and L. David, "Optimization of log-periodic dipole antennas," *IEEE Trans. Antennas Propagat.*, vol. AP-19, pp. 286–288, Mar. 1971.
[15] J. N. Nkeng, "Asymmetry anomalies of log-periodic dipole antennas," M.A.Sc. thesis, Dept. of Elect. Engineering, Univ. of Toronto, Toronto, Ont., Canada, July 1975.
[16] W. A. Imbriale, private communication.
[17] R. H. Kyle, "Mutual coupling between log-periodic antennas," *IEEE Trans. Antennas Propagat.*, vol. AP-18, pp. 15–22, Jan. 1970.
[18] C. Elfving and S. Miller, "Gain variations in E-plane arrays of log-periodic antennas," Tech. Rpt. ECOM-0503-P005-G815, Sylvania Electronic Systems West, Mountain View, Calif., Nov. 1969.
[19] S. C. Kuo, "Size-reduced log-periodic dipole array," *Digest 1970 IEEE/G-AP Int. Symp.*, pp. 151–158.